ELSEVIER

Journal of Organometallic Chemistry 633 (2001) 7–17

Journal of Organometallic Chemistry

www.elsevier.com/locate/jorganchem

Synthesis and characterization of triorganotin(IV) complexes of 5-[(*E*)-2-(aryl)-1-diazenyl]-2-hydroxybenzoic acids. Crystal and molecular structures of a series of triphenyltin 5-[(*E*)-2-(aryl)-1-diazenyl]-2-hydroxybenzoates (aryl = phenyl, 2-methylphenyl, 3-methylphenyl and 4-methoxyphenyl)

Tushar S. Basu Baul [a,*], Sushmita Dhar [a], Simon M. Pyke [b], Edward R.T. Tiekink [b,*], Eleonora Rivarola [c], Ray Butcher [d], Frank E. Smith [e,*]

[a] *Chemical Laboratory, Regional Sophisticated Instrumentation Centre, North-Eastern Hill University, Bijni Complex, Bhagyakul, Shillong 793 003, India*

[b] *Department of Chemistry, The University of Adelaide, Adelaide, South Australia 5005, Australia*

[c] *Dipartimento di Chimica Inorganica, Universita di Palermo, Palermo 90123, Italy*

[d] *Department of Chemistry, Howard University, Washington, DC 20059, USA*

[e] *School of Graduate Studies and Research, Laurentian University, Sudbury, Ont., Canada P3E 2C6*

Received 18 October 2000; received in revised form 6 March 2001; accepted 13 March 2001

Abstract

The triphenyltin and tri-*n*-butyltin complexes of some 5-[(*E*)-2-(aryl)-1-diazenyl]-2-hydroxybenzoic acids have been synthesized and characterized by ^{1}H-, ^{13}C-, ^{119}Sn-NMR, IR and ^{119m}Sn Mössbauer spectroscopic techniques in combination with elemental analysis. The crystal structures of triphenyltin 5-[(*E*)-2-(aryl)-1-diazenyl]-2-hydroxybenzoates (aryl = phenyl, 2-methylphenyl, 3-methylphenyl and 4-methoxyphenyl) are reported. Both X-ray and ^{119}Sn Mössbauer data indicate that the triphenyltin complexes adopt a monomeric distorted tetrahedral configuration with the carboxylate ligand coordinating in a monodentate mode. By contrast, ^{119}Sn Mössbauer spectroscopy shows that each tributyltin complex is polymeric and features a trans-trigonal bipyramidal geometry with a planar $SnBu_3$ unit and two apical carboxylate oxygen atoms derived from bidentate bridging carboxylate ligands. This is a solid-state effect, as both ^{119}Sn-NMR and $^{1}J(^{13}C-^{119/117}Sn)$ coupling constant data indicate tetrahedral geometries in solution for the triphenyl and tri-*n*-butyl complexes.

Keywords: Organotin; Carboxylates; 5-[(*E*)-2-(Aryl)-1-diazenyl]-2-hydroxybenzoic acids; NMR; Mössbauer; X-ray

1. Introduction

Triorganotin compounds have been the subject of interest for some time because of their biomedical and commercial applications. Tributyltin, in the form of halides, oxides and acetates, displays a large array of biocidal properties and is used extensively in wood preservatives and in marine anti-fouling paints [1], although there has been considerable environmental concern about their latter use [2]. However, the tributyltin compounds have not been shown to be neurotoxins, mutagens, teratogens, or carcinogens in humans [3]. Triphenyltin compounds, including triphenyltin acetate, have achieved commercialization as agricultural fungicides [4–8]. In addition to their commercial applications, triorganotin carboxylates present an interesting variety of structural possibilities [9,10]. Much current organotin research is concentrated on their biomedical applications, particularly their anticancer properties. Against human tumour cell lines, triphenyltin derivatives are highly active, being characterized by very low ID_{50} values [11]. In general, triorganotin compounds display a higher biological activity than their di- and

* Corresponding authors. Fax: +91-364-228213.
E-mail address: basubaul@hotmail.com (T.S. Basu Baul).

PII: S0022-328X(01)01024-5

mono-organotin analogues. This has been attributed to their ability to bind proteins [12–14]. For this reason, a number of triphenyltin salicylates have been synthesized [15–17] and screened against human tumour cell lines (MCF-7 and WiDr). The results were found to be comparable with those of mitomycin C [17]. In line with these developments, we have recently reported some triorganotin complexes of azo-salicylic acid [18]. As a continuation of this line of investigation, we now describe some triphenyltin and tri-*n*-butyltin complexes derived from a number of 5-[(*E*)-2-(aryl)-1-diazenyl]-2-hydroxybenzoic acids, since the structural motif and activity are likely to be influenced by a steric effect associated with the carboxylate residue. The generic structure of the acid is shown in Fig. 1.

2. Experimental

2.1. Materials

$(Bu_3Sn)_2O$ (Merck), Ph_3SnCl (Fluka AG), salicylic acid (Merck) and the substituted anilines (reagent grade) were used without further purification. All the solvents used in the reactions were of AR grade and dried using standard literature procedures.

2.2. Physical measurements

Carbon, hydrogen and nitrogen analyses were performed with a Perkin–Elmer 2400 series II instrument. IR spectra in the range 4000–400 cm^{-1} were obtained on a Perkin–Elmer 983 spectrophotometer with samples investigated as KBr discs. The ^{1}H- and ^{13}C-NMR spectra of the ligands were acquired on either a Varian Gemini 2000 spectrometer (operating at 300.13 and 75.47 MHz respectively) or a Varian Inova spectrometer (operating at 599.91 and 150.85 MHz respectively). For the organotin compounds, the ^{1}H-, ^{13}C- and ^{119}Sn-NMR spectra were recorded on a Bruker ACF 300 spectrometer and measured at 300.13, 75.47 and 111.92 MHz respectively. The ^{1}H, ^{13}C and ^{119}Sn chemical shifts were referred to Me_4Si set at 0.00 ppm, $CDCl_3$ set at 77.0 ppm and tetramethyltin set at 0.00 ppm respectively. ^{119}Sn Mössbauer spectra of the complexes in the solid state were recorded on an Elscient–Laben spectrometer equipped with an AERE cryostat at liquid-nitrogen temperature. The $Ca^{119m}SnO_3$ Mössbauer source (10 mCi; Radiochemical Centre, Amersham, UK) moved with constant acceleration and triangular waveform. The velocity calibration was made using a ^{57}Co Mössbauer source (10 mCi). An iron foil enriched to 95% in ^{57}Fe (DuPont Pharma Italia, Firenze, Italy) was used as the absorber.

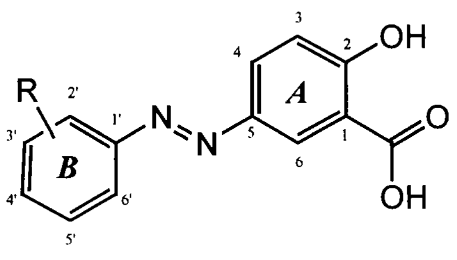

Fig. 1. Generic structure of the acid. Abbreviations: L^1HH': R = H; L^2HH': R = 2′-CH_3; L^3HH': R = 3′-CH_3; L^4HH': R = 4′-CH_3; L^5HH': R = 4′-Br; L^6HH': R = 4′-NO_2; L^7HH': R = 4′-OCH_3, where H and H′ represent hydroxyl and carboxyl protons, respectively.

2.3. Synthesis of 5-[(E)-2-(aryl)-1-diazenyl]-2-hydroxybenzoic acids

A typical procedure is described below.

2.3.1. Preparation of 5-[(E)-2-phenyl-1-diazenyl]-2-hydroxybenzoic acid (L^1HH')

Aniline (5.0 g, 53.8 mmol) was mixed with HCl (16 ml) and water (16 ml) and digested in a water bath for 30 min. The hydrochloride was cooled to 5 °C and diazotized with ice-cold aqueous $NaNO_2$ solution (3.7 g, 20 ml). A cold solution of salicylic acid (7.42 g, 53.8 mmol), previously dissolved in 10% NaOH soution (50 ml), was then added to the cold diazonium salt solution with vigorous stirring. A yellow colour developed almost immediately and the stirring was continued for 1 h. The reaction mixture was kept overnight in a refrigerator, followed by 3 h. at room temperature, and then acidified with dilute acetic acid, whereupon a yellow precipitate separated out. The precipitate was filtered, washed several times with water to remove excess acetic acid and water-soluble materials, and then dried in air. The crude product was washed with hexane to remove any tarry materials and recrystallized from methanol to yield pure L^1HH' (4.72 g, 33%). M.p.: 212–214 °C. Anal. Found: C, 64.30; H, 4.10; N, 11.46. Calc. for $C_{13}H_{10}N_2O_3$: C, 64.46; H, 4.16; N, 11.57%. ^{1}H-NMR (DMSO-d_6/600 MHz); δ_H: 6.98 [d, 8.4 Hz, 1H, H3], 7.46 [m, 1H, H4′], 7.50 [m, 2H, H3′ & H5′], 7.81 [m, 2H, H2′ & H6′], 7.94 [dd, 8.4 & 2.4 Hz, 1H, H4], 8.29 [d, 2.4 Hz, 1H, H6] ppm. Signals for the phenol and carboxylic acid were exchanged due to presence of water in the solvent. ^{13}C-NMR (DMSO-d_6/150 MHz); δ_C: 116.3 [C1], 118.1 [C3], 122.3 [C2′ & C6′], 125.9 [C6], 128.4 [C4], 129.5 [C3′ & C5′], 130.7 [C4′], 143.8 [C5], 152.1 [C1′], 165.7 [C2], 171.3 [CO_2H] ppm.

The other 5-[(*E*)-2-(aryl)-1-diazenyl]-2-hydroxybenzoic acids, viz. L^2HH'–L^7HH' were prepared analogously with appropriate anilines and their analytical data are presented below. Note: the quantities of HCl and NaOH used for the preparations were found to be important. Quantities less than those specified produced either oils or unidentified products. The quantities of HCl and NaOH (10%) used were as follows. For L^2HH'–L^4HH': 12 ml and 31 ml; for L^5HH': 9 ml and 36.7 ml; for L^6HH': 9 ml and 28 ml; and for L^7HH': 9 ml and 35.5 ml, HCl and NaOH respectively.)

2.3.2. 5-[(E)-2-(2-Methylphenyl)-1-diazenyl]-2-hydroxybenzoic acid (L^2HH')

Recrystallized from methanol to give brown precipitate in 50% yield. M.p.: 190–191 °C. Anal. Found: C, 65.50; H, 4.57; N, 11.01. Calc. for $C_{14}H_{12}N_2O_3$: C, 65.63; H, 4.72; N, 10.93%. ^{1}H-NMR (DMSO-d_6/600 MHz); δ_H: 2.64 [s, 3H, CH_3], 7.14 [d, 9.0 Hz, 1H, H3], 7.30 [m, 1H, H5′], 7.41 [m, 2H, H3′ & H4′], 7.55 [d, 7.8 Hz, 1H, H6′], 8.06 [dd, 9.0 & 2.4 Hz, 1H, H4], 8.32 [d, 2.4 Hz, 1H, H6] ppm. Signals for the phenol and carboxylic acid were exchanged due to presence of water in the solvent. ^{13}C-NMR (DMSO-d_6/150 MHz); δ_C: 17.0 [CH_3], 113.6 [C1], 115.1 [C6′], 118.3 [C3], 126.3 [C6], 126.6 [C5′], 128.3 [C4], 130.9 [C4′], 131.3 [C3′], 137.2 [C2′], 144.9 [C5], 149.8 [C1′], 163.4 [C2], 171.3 [CO_2H] ppm.

2.3.3. 5-[(E)-2-(3-Methylphenyl)-1-diazenyl]-2-hydroxybenzoic acid (L^3HH')

Recrystallized from methanol to give yellow precipitate in 50% yield. M.p.: 196–198 °C. Anal. Found: C, 65.55; H, 4.70; N, 10.85. Calc. for $C_{14}H_{12}N_2O_3$: C, 65.63; H, 4.72; N, 10.93%. ^{1}H-NMR (DMSO-d_6/600 MHz); δ_H: 2.40 [s, 3H, CH_3], 7.14 [d, 9.0 Hz, 1H, H3], 7.34 [dquin, 7.2 & 1.0 Hz, 1H, H4′], 7.45 [t, 7.2 Hz, 1H, H5′], 7.66 [m, 2H, H2′ & H6′], 8.06 [dd, 9.0 & 2.4 Hz, 1H, H4], 8.31 [d, 2.4 Hz, 1H, H6] ppm. Signals for the phenol and carboxylic acid were exchanged due to presence of water in the solvent. ^{13}C-NMR (DMSO-d_6/150 MHz); δ_C: 20.8 [CH_3], 113.6 [C1], 118.3 [C3], 119.9 [C6′], 122.4 [C2′], 125.6 [C6], 128.8 [C4], 129.1 [C5′], 131.7 [C4′], 138.8 [C3′], 144.5 [C5], 151.8 [C1′], 163.4 [C2], 171.3 [CO_2H] ppm.

2.3.4. 5-[(E)-2-(4-Methylphenyl)-1-diazenyl]-2-hydroxybenzoic acid (L^4HH')

Recrystallized from methanol to give yellow precipitate in 50% yield. M.p.: 217–218 °C. Anal. Found: C, 65.51; H, 4.63; N, 10.80. Calc. for $C_{14}H_{12}N_2O_3$: C, 65.63; H, 4.72; N, 10.93%. ^{1}H-NMR (DMSO-d_6/300 MHz); δ_H: 2.41 [s, 3H, CH_3], 7.06 [d, 9.0 Hz, 1H, H3], 7.31 [AA′ portion of AA′XX′, 2H, H2′ & H6′], 7.78 [XX′ portion of AA′XX′, 2H, H3′ & H5′], 8.05 [dd, 9.0 & 2.1 Hz, 1H, H4], 8.48 [d, 2.1 Hz, 1H, H6] ppm. Signals for the phenol and carboxylic acid were exchanged due to presence of water in the solvent. ^{13}C-NMR (DMSO-d_6/75 MHz); δ_C: 20.7 [CH_3], 112.4 [C1], 117.3 [C3], 121.8 [C2′ & C6′], 126.3 [C6], 127.6 [C4], 129.0 [C3′ & C5′], 140.4 [C4′], 144.4 [C5], 149.7 [C1′], 163.3 [C2], 171.7 [CO_2H] ppm.

2.3.5. 5-[(E)-2-(4-Bromophenyl)-1-diazenyl]-2-hydroxybenzoic acid (L^5HH')

Recrystallized from methanol to give brown precipitate in 50% yield. M.p.: 242–244 °C. Anal. Found: C, 48.59; H, 2.80; N, 8.68. Calc. for $C_{13}H_9BrN_2O_3$: C, 48.63; H, 2.83; N, 8.72%. ^{1}H-NMR (DMSO-d_6/300 MHz); δ_H: 7.04 [d, 9.0 Hz, 1H, H3], 7.63 [AA′ portion of AA′XX′, 2H, H2′ & H6′], 7.78 [XX′ portion of AA′XX′, 2H, H3′ & H5′], 8.04 [dd, 9.0 & 2.1 Hz, 1H, H4], 8.45 [d, 2.1 Hz, 1H, H6] ppm. Signals for the phenol and carboxylic acid were exchanged due to presence of water in the solvent. ^{13}C-NMR (DMSO-d_6/75 MHz); δ_C: 113.2 [C1], 118.1 [C3], 124.1 [C2′ & C6′], 124.6 [C6], 127.4 [C4], 128.3 [C4′], 132.2 [C3′ & C5′], 144.8 [C5], 151.0 [C1′], 164.5 [C2], 172.2 [CO_2H] ppm.

2.3.6. 5-[(E)-2-(4-Nitrophenyl)-1-diazenyl]-2-hydroxybenzoic acid (L^6HH')

Recrystallized from methanol to give orange–red precipitate in 49% yield. M.p.: 234–236 °C. Anal. Found: C, 54.28; H, 3.25; N, 14.78. Calc. for $C_{13}H_9N_3O_5$: C, 54.37; H, 3.16; N, 14.63%. ^{1}H-NMR (DMSO-d_6/300 MHz); δ_H: 6.64 [d, 9.0 Hz, 1H, H3], 7.60 [AA′ portion of AA′XX′, 2H, H2′ & H6′], 7.66 [XX′ portion of AA′XX′, 2H, H3′ & H5′], 7.96 [dd, 9.0 & 2.1 Hz, 1H, H4], 8.08 [d, 2.1 Hz, 1H, H6] ppm. Signals for the phenol and carboxylic acid were exchanged due to the presence of water in the solvent. ^{13}C-NMR (DMSO-d_6/75 MHz); δ_C: 113.6 [C1], 118.2 [C3], 123.2 [C2′ & C6′], 124.6 [C3′ & C5′], 125.6 [C6], 128.4 [C4], 144.7 [C4′], 148.3 [C5], 155.4 [C1′], 165.5 [C2], 172.0 [CO_2H] ppm.

2.3.7. 5-[(E)-2-(4-Methoxyphenyl)-1-diazenyl]-2-hydroxybenzoic acid (L^7HH')

Recrystallized from methanol to give brown precipitate in 52% yield. M.p.: 209–210 °C. Anal. Found: C, 61.60; H, 4.41; N, 10.35. Calc. for $C_{14}H_{12}N_2O_4$: C, 61.77; H, 4.44; N, 10.29%. ^{1}H-NMR (DMSO-d_6/300 MHz); δ_H: 3.86 [s, 3H, OCH_3], 7.02 [d, 9.0 Hz, 1H, H3], 7.06 [AA′ portion of AA′XX′, 2H, H2′ & H6′], 7.84 [XX′ portion of AA′XX′, 2H, H3′ & H5′], 8.00 [dd, 9.0 & 2.1 Hz, 1H, H4], 8.35 [d, 2.1 Hz, 1H, H6] ppm. Signals for the phenol and carboxylic acid were exchanged due to presence of water in the solvent. ^{13}C-NMR (DMSO-d_6/75 MHz); δ_C: 54.0 [OCH_3], 111.7 [C1], 112.8 [C2′ & C6′], 116.5 [C3], 122.9 [C3′ & C5′], 124.5 [C6], 126.8 [C4], 143.3 [C4′], 144.8 [C5], 160.2 [C1′], 162.0 [C2], 170.6 [CO_2H] ppm. Recrystallization of L^7HH' from benzene solution gave orange–red crystals suitable for X-ray crystallography; results have been reported elsewhere [19].

2.4. Preparation of sodium salts of 5-[(E)-2-(aryl)-1-diazenyl]-2-hydroxybenzoic acids (LHNa)

The sodium salts of 5-[(*E*)-2-(aryl)-1-diazenyl]-2-hydroxybenzoic acids, viz. L^1HNa–L^7HNa, were prepared by reacting stoichiometric amounts of the acids with a slight excess of $NaHCO_3$ in water. The reaction mixture was heated on a hot plate until the dissolution was complete and filtered while hot. The filtrate was evaporated on the water bath to dryness. The dry residue was extracted with anhydrous methanol and the solvent was distilled off. The residue was then washed with diethyl ether and dried in vacuo prior to its use for the preparation of the triphenyltin complexes.

2.5. Preparation of 5-[(E)-2-(4-chlorophenyl)-1-diazenyl]-2-hydroxymethylbenzoate, LHMe

5-[(*E*)-2-(4-Chlorophenyl)-1-diazenyl]-2-hydroxybenzoic acid [18] (0.56 g) was dissolved in anhydrous methanol (20 ml) and refluxed for 5 h with concentrated H_2SO_4 (0.6 ml). The solvent was distilled off and the residue was dissolved in diethyl ether and washed with water to remove any acid. The ether extract was passed through anhydrous Na_2SO_4 and the filtrate was evaporated to dryness. The yellow-coloured methylated product was dried in vacuo. Yield: 90%; m.p.: 152–153 °C. Anal. Found: C, 57.79; H, 3.89; N, 10.02. Calc. for $C_{14}H_{11}ClN_2O_3$: C, 57.85; H, 3.81; N, 9.64%. ^{1}H-NMR ($CDCl_3$/300 MHz); δ_H: 4.02 [s, 3H, OCH_3], 7.08 [d, 9.0 Hz, 1H, H3], 7.46 [AA′ portion of AA′XX′, 2H, H2′ & H6′], 7.82 [XX′ portion of AA′XX′, 2H, H3′ & H5′], 8.06 [dd, 9.0 & 2.1 Hz, 1H, H4], 8.42 [d, 2.1 Hz, 1H, H6], 11.08 [brs, 1H, OH] ppm. ^{13}C-NMR ($CDCl_3$/75 MHz); δ_C: 52.3 [OCH_3], 112.1 [C1], 118.4 [C3], 123.8 [C2′ & C6′], 126.9 [C6], 128.6 [C4], 129.1 [C3′ & C5′], 136.5 [C4′], 144.7 [C5], 157.5 [C1′], 164.1 [C2], 170.0 [CO_2] ppm.

2.6. Synthesis of the triorganotin complexes

Two typical methods are described below.

2.6.1. Synthesis of Ph_3SnL^1H

Ph_3SnCl (0.50 g, 1.30 mmol) in methanol (30 ml) was added dropwise with continuous stirring to a hot methanol solution (50 ml) containing L^1HNa (0.34 g, 1.30 mmol). The reaction mixture was then refluxed for 5 h and the solvent was removed using a rotary evaporator. The residue was washed with hexane, extracted into chloroform and filtered. The crude product was obtained after evaporation of the chloroform. This was then recrystallized from a large volume of hot hexane to yield orange blocks of the desired product at room temperature.

2.6.2. Synthesis of Bu_3SnL^2H

The compound was synthesized by mixing L^2HH' (0.50 g, 1.95 mmol) and $(Bu_3Sn)_2O$ (0.58 g, 0.97mmol) in 50 ml of anhydrous toluene, in a 100 ml flask equipped with a Dean–Stark moisture trap and a water-cooled condenser. The mixture was refluxed for 3 h. The solvent was distilled off to half of the initial solvent volume. The remaining solvent was removed using a rotary evaporator. The dark-red oil that remained was dissolved in 20 ml of petroleum ether (40–60 °C) and triturated under cold conditions. A dark-red solid was obtained upon refrigeration. The crude product was recrystallized from petroleum ether, which yielded dark-red solid upon refrigeration for several days.

2.7. X-ray crystallography

Crystallographic data, collection and refinement details are given in Table 1. Corrections for absorption were made using a semi-empirical method 20a for **1** and **3** and an empirical procedure [20b] for **5** and **12**. The structures were solved by heavy-atom methods [20c] and refined by a full-matrix least-squares procedure based on F^2 (**1** and **3**) or F (**5** and **12**) [20d]. Non-hydrogen atoms were refined employing anisotropic displacement parameters and hydrogen atoms were included in the models at their calculated positions. The hydroxyl hydrogen atom was located from a difference map in each case. The weighting scheme employed for **1** was of the form $w = 1/[\sigma^2(F) + (0.0308P)^2 + 0.6912P]$, where $P = (F_o^2 + 2F_c^2)/3$, $w = 1/[\sigma^2(F) + (0.0319P)^2 + 1.3971P]$ for **3**, and $w = 1/[\sigma^2(F) + g|F_o|^2]$ ($g = 0.000\,04$ for **5** and $g = 0.000\,05$ for **12**). The absolute structure of **12** was not determined, as there were no significant differences in measured Friedel pairs included in the data set. The structures of **1**, **3** and **12** each feature multiple independent molecules, i.e. two, two and four, in their respective asymmetric units. No evidence was found for additional symmetry in these structures that would reduce the number of independent molecules [20d,e]. The molecular structures, showing the crystallographic numbering schemes employed, are shown in Figs. 2–5 and were drawn with ORTEP at the 35% (**1** and **3**) and 50% (**5** and **12**) probability levels, respectively [20f]. PLATON [20e] was employed in the analysis of the crystal structures.

3. Results and discussion

3.1. Syntheses

The 5-[(*E*)-2-(aryl)-1-diazenyl]-2-hydroxybenzoic acid ligands were prepared by the diazonium coupling reaction between the appropriate anilines and salicylic acid in alkaline medium under cold conditions. The basic

Table 1
Crystallographic data and structure refinement parameters for the triorganotin complexes **1**, **3**, **5** and **12**

	1	**3**	**5**	**12**
Empirical formula	$C_{31}H_{24}N_2O_3Sn$	$C_{32}H_{26}N_2O_3Sn$	$C_{32}H_{26}N_2O_3Sn$	$C_{32}H_{26}N_2O_4Sn$
Formula weight	591.2	605.3	605.3	621.3
Diffractometer	Rigaku AFC6S	Rigaku AFC6S	Rigaku AFC7R	Rigaku AFC7R
Temperature (K)	293	293	173	173
Crystal system	Triclinic	Triclinic	Monoclinic	Monoclinic
Space group	$P\bar{1}$	$P\bar{1}$	$P2_1/c$	$P2_1$
a (Å)	11.4219(11)	11.1765(15)	12.534(2)	10.595(2)
b (Å)	13.8246(13)	14.538(2)	16.467(2)	19.692(4)
c (Å)	18.711(2)	18.485(3)	13.334(4)	27.305(2)
α (°)	105.627(6)	105.688(12)	90	90
β (°)	91.646(7)	93.007(11)	101.33(2)	100.19(1)
γ (°)	100.900(7)	98.215(8)	90	90
V (Å^3)	2784.0(5)	2848.9(7)	2698.7(9)	5607(1)
Z	4	4	4	8
D_x (g cm^{-3})	1.411	1.411	1.490	1.472
μ (cm^{-1})	9.51	9.31	9.83	9.51
Reflections measured	12 773	12 631	6699	13 941
θ_{max} (°)	27.5	27.5	27.5	27.5
Unique reflections	12 629	12 006	6418	13 243
Refined parameters	722	745	343	1404
Reflections with $I \geq n\sigma(I)$	9311, $n=2$	9563, $n=2$	4190, $n=3$	7843, $n=3$
R [a]	0.054	0.046	0.027	0.039
R_w^a	0.087	0.092	0.030	0.034
ρ_{max} (e$^-$ Å^{-3})	0.28	0.55	0.28	0.48

[a] All reflections.

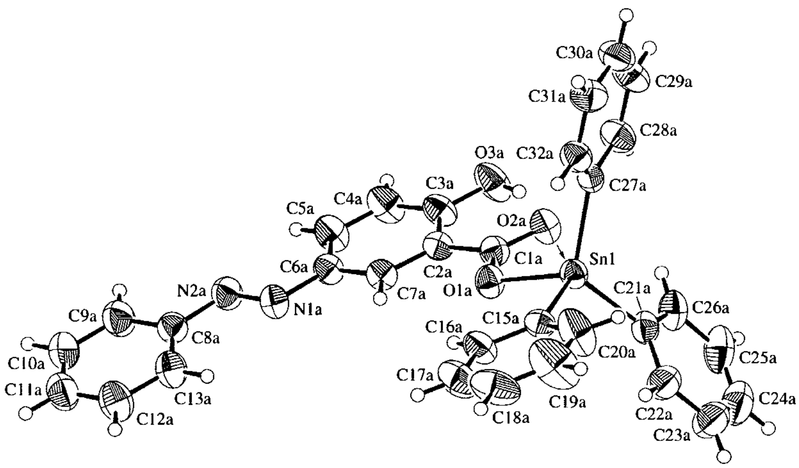

Fig. 2. Molecular structure and crystallographic numbering scheme for **1**.

ligand framework is shown in Fig. 1, along with the abbreviations of the ligands and numbering scheme for spectroscopic analysis. The details of their synthesis and characterization are presented in Section 2.

The new organotin complexes are abbreviated as R_3SnLH, where R = phenyl or n-butyl. They were obtained either from the reaction of sodium salts of the ligands with Ph_3SnCl in methanol solution or by the condensation of the appropriate ligands with $(Bu_3Sn)_2O$ in toluene solution. The influence of different substituents on phenyl ring B did not cause obvious variation in the yield of the reaction. The characterization data of the complexes are listed in Table 2. These confirm the formulation of the products. They are stable in air and are soluble in all common organic solvents.

3.2. IR data

Diagnostically important IR absorption frequencies for the carboxylic antisymmetric [ν_{asym}(OCO)] stretching vibration are shown in Table 3. The assignment of the symmetric [ν_{sym}(OCO)] stretching vibration band could not be made owing to the complex pattern of the spectra. The assignment of the band is based on comparison with the spectra of the free ligands (LHH′), their sodium salts (LHNa) and also, in one case, by comparison with the methylated product (LHMe). The antisymmetric [ν_{asym}(OCO)] stretching vibrations for the uncomplexed ligands have been detected in the 1652–1670 cm^{-1} region. The lower value of this absorption band, compared with the methyl ester, is due

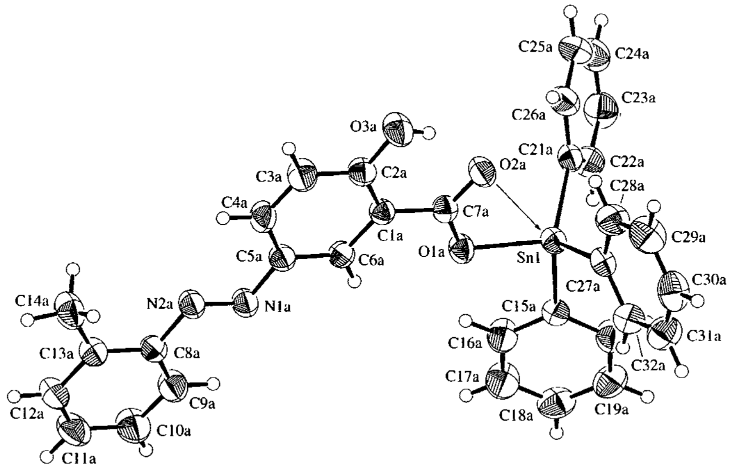

Fig. 3. Molecular structure and crystallographic numbering scheme for **3**.

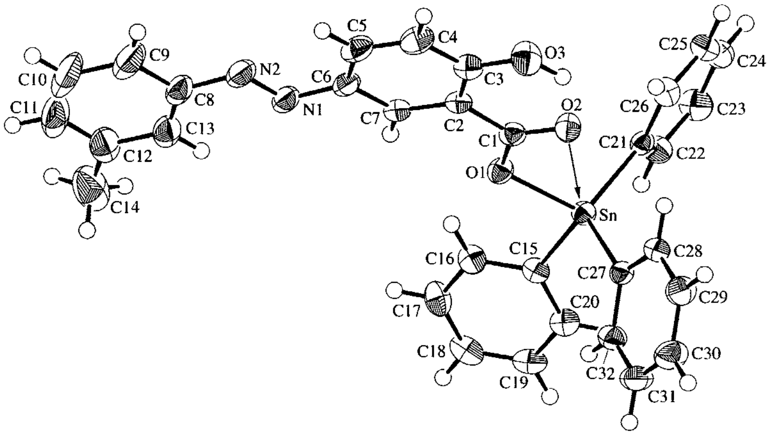

Fig. 4. Molecular structure and crystallographic numbering scheme for **5**.

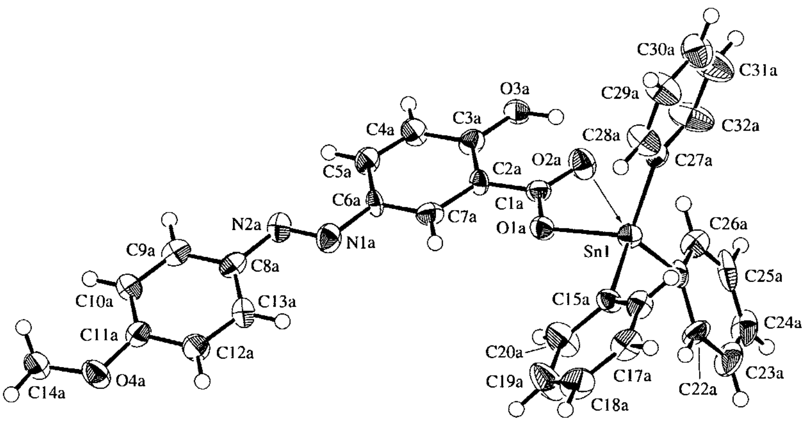

Fig. 5. Molecular structure and crystallographic numbering scheme for **12**.

Table 2
Characterization data for the triorganotin complexes

Complex	Crystallization solvent	Colour	Yield (%)	M.p. (°C)	Elemental analysis, found (calc.) (%)		
					C	H	N
Ph_3SnL^1H (**1**)	Hexane	Orange	63	136–138	62.9 (62.98)	4.00 (4.09)	4.80 (4.74)
Bu_3SnL^1H (**2**)	Petroleum ether	Yellow	60	32–34	56.50 (56.52)	6.70 (6.83)	5.30 (5.27)
Ph_3SnL^2H (**3**)	Hexane	Orange	50	158–160	63.50 (63.50)	4.50 (4.33)	4.60 (4.63)
Bu_3SnL^2H (**4**)	Petroleum ether	Brick-red	89	42–44	57.40 (57.27)	7.00 (7.02)	5.14 (5.14)
Ph_3SnL^3H (**5**)	Hexane	Orange	40	140–141	63.48 (63.50)	4.33 (4.33)	4.70 (4.63)
Bu_3SnL^3H (**6**)	Petroleum ether	Brick-red	61	46–48	57.30 (57.27)	7.06 (7.02)	5.20 (5.14)
Ph_3SnL^4H (**7**)	Hexane	Orange	52	140–141	63.50 (63.50)	4.50 (4.33)	4.60 (4.63)
Bu_3SnL^4H (**8**)	Petroleum ether	Light-orange	82	35–36	57.30 (57.27)	7.00 (7.02)	5.26 (5.14)
Bu_3SnL^5H (**9**)	Petroleum ether	Yellow	83	38–40	49.00 (49.21)	5.70 (5.78)	4.60 (4.59)
Ph_3SnL^6H (**10**)	Hexane	Orange	40	138–140	58.50 (58.53)	3.60 (3.64)	6.75 (6.60)
Bu_3SnL^6H (**11**)	Petroleum ether	Orange–red	93	36–38	52.24 (52.11)	6.00 (6.12)	7.32 (7.29)
Ph_3SnL^7H (**12**)	Hexane	Orange	47	150–152	61.50 (61.87)	4.22 (4.22)	4.50 (4.51)
Bu_3SnL^7H (**13**)	Petroleum ether	Yellow	50	34–36	55.67 (55.64)	6.80 (6.82)	5.08 (4.99)

Table 3
IR data [ν_{asym}(OCO)] (cm^{-1}) for the ligands (LHH′), sodium salts (LHNa) and triorganotin complexes (R_3SnLH) [a]

LHH′	IR	LHNa	IR	Ph_3SnLH	IR	Bu_3SnLH	IR
L^1HH'	1659	L^1HNa	1583	**1**	1586	**2**	1637
L^2HH'	1668	L^2HNa	1583	**3**	1589	**4**	1618
L^3HH'	1652	L^3HNa	1583	**5**	1588	**6**	1620
L^4HH'	1653	L^4HNa	1583	**7**	1587	**8**	1590
L^5HH'	1657	L^5HNa	1587	–	–	**9**	1637
L^6HH'	1675	L^6HNa	1588	**10**	1622	**11**	1636
L^7HH'	1673	L^7HNa	1587	**12**	1600	**13**	1630

[a] Complex numbers as shown in Table 2.

to the strong intramolecular hydrogen bonding established between the OH and COOH groups of ring A [18]. For example, for 5-[(*E*)-2-(4-chlorophenyl)-1-diazenyl]-2-hydroxybenzoic acid ν_{asym}(OCO) is at 1658 cm^{-1} and at 1670 cm^{-1} for 5-[(*E*)-2-(4-chlorophenyl)-1-diazenyl]-2-hydroxy methyl benzoate. In the complexes, the carbonyl stretching frequencies are found to be shifted to lower wavenumber, which is ascribed to carboxylate coordination in accord with earlier reports [18]. It should be noted that intramolecular O–H···O hydrogen bonding involving ring A is also present in the solid state, as revealed by the results of the X-ray crystallographic study (see Section 3.5).

3.3. ^1H-, ^{13}C- and ^{119}Sn-NMR data

The ^1H-NMR data of the ligands are given in Section 2. The signals were assigned by the use of correlated spectroscopy (COSY), heteronuclear single-quantum correlation (HSQC) and Constant time Inverse-detection Gradient Accordion Rescaled (CIGAR) heteronuclear multiple-bond connectivities (HMBC) [21] experiments using gradient coherence selection. Rotating-frame Overhauser enhancement spectroscopy (ROESY) spectra were required in order to assign the aromatic protons adjacent to the methyl groups of ligands (in L^2HH' and L^3HH') due to overlapped B ring signals in the ^1H-NMR spectra (in the case of L^2HH', the B ring ^1H signals were severely distorted due to very similar chemical shifts for H3 and H4). The conclusions drawn from the ligand assignments were then extrapolated to the complexes owing to the data similarity. The ^1H and ^{13}C chemical shift assignment (Tables 4 and 5 respectively) of the triorganotin moiety is straightforward from the multiplicity patterns, resonance intensities and also by examining the $^nJ(^{13}C-^{119/117}Sn)$ coupling constants [18,22]. The ^1H-NMR integration values were completely consistent with the formulation of the products.

Holeček and coworkers [23–26] have shown that the $^1J(^{13}C-^{119/117}Sn)$ coupling constants can be used as an indicator of the coordination number of the tin atom in triorganotin compounds. Four-coordinated triphenyltin compounds exhibit couplings in the range 550–650 Hz and five-coordinated analogues in the range 750–850 Hz. Four-coordinated tributyltin compounds, however, exhibit couplings in the range 325–390 Hz, and five-coordinated ones in the range 440–540 Hz. The

Table 4
^{1}H-NMR data (δ, ppm) for the triorganotin complexes in $CDCl_3$

Compound	Ligand skeleton [a]										Sn–R skeleton [b]			
	113	114	116	H2′	H3′	H4′	H5′	H6′	R	OH	1*	2*	3*	4*
1	7.05	7.86	8.62	7.82	7.49	7.49	7.49	7.82	–	11.57	–	7.82	7.49	7.49
2	7.03	8.04	8.51	7.87	7.45	7.38	7.45	7.87	–	11.95	1.68	1.38	1.38	0.95
3	6.95	7.96	8.58	–	7.21	7.21	7.18	7.60	2.69	11.33	–	7.76	7.43	7.43
4	7.02	8.00	8.47	–	7.26	7.26	7.20	7.62	2.70	11.94	1.68	1.38	1.38	0.94
5	6.94	7.98	8.57	7.63	–	7.12	7.26	7.63	2.44	11.34	–	7.70	7.38	7.38
6	6.99	8.00	8.43	7.65	–	7.18	7.31	7.65	2.44	11.77	1.67	1.38	1.38	0.96
7	6.88	7.94	8.53	7.11	7.37	–	7.37	7.11	2.34	11.30	–	7.70	7.37	7.37
8	7.02	8.02	8.46	7.23	7.77	–	7.77	7.23	2.40	11.89	1.69	1.39	1.39	0.93
9	7.01	8.00	8.45	7.58	7.74	–	7.74	7.58	–	11.93	1.70	1.39	1.39	0.95
10	7.02	8.33	8.64	7.47	8.04	–	8.04	7.47	–	11.59	–	7.76	7.47	7.47
11	7.02	8.34	8.51	7.97	8.04	–	8.04	7.97	–	12.01	1.71	1.40	1.40	0.97
12	6.92	7.99	8.54	6.98	7.84	–	7.84	6.98	3.64	11.38	–	7.77	7.46	7.46
13	6.96	8.02	8.47	7.03	7.86	–	7.86	7.03	3.88	11.95	1.70	1.40	1.40	0.95

[a] Refer to Fig. 1. for numbering scheme. No change is observed in the multiplicity and coupling constants when compared with the respective ligands. OH signal is broad singlet in all cases.

[b] Numbering scheme for Sn–R skeleton as shown below:

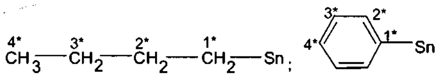

The signals due to Sn–R protons were multiplets except for 4* of Sn–Bu_3 complexes, which is triplet, and the coupling constant was 7 Hz.

triorganotin complexes of the present investigation exhibit $^{1}J(^{13}C-^{119/117}Sn)$ coupling satellites of the order of 645 Hz in the case of triphenyltin and 335 Hz in the tri-*n*-butyltin complexes in $CDCl_3$ solution, suggesting that the tin atom is four-coordinate in solution. In the case of the tributyltin complexes, a polymeric structure is possible in the solid state (see Section 3.4) [22]; this is possibly lost in solution to generate a monomeric four-coordinated tetrahedral structure. Further, the ^{13}C chemical shift of the *ipso*-carbon (C1*) of the Sn–Ph_3 moiety is around 138 ppm (see Table 5), which is also characteristic for a tetrahedral tin atom [27], since for five-coordinated triphenyltin carboxylates a value at approximately 4 ppm higher frequency is found.

The ^{119}Sn-NMR chemical shifts of triorganotin complexes in $CDCl_3$ solution are listed in Table 6. The complexes exhibit a single sharp resonance in the ranges -86.9 to -91.6 ppm (triphenyltin) and 130.8 to 138.7 ppm (tri-*n*-butyltin) consistent with the range specified for tetrahedral triorganotin compounds [24]. This is further supported by recent work on analogous triorganotin azocarboxylates [18,22]. The ^{119}Sn-NMR chemical shifts show obvious dependence on the nature of the substituents in the ligand B rings, whereas $\delta(^{13}C)$ chemical shifts of the carbon atoms of the triorganotin group and the values of $^{n}J(^{13}C-^{119/117}Sn)$ coupling constants are not affected.

3.4. ^{119}Sn Mössbauer data

The Mössbauer spectra of some representative triorganotin complexes have been recorded (Table 6) in order to obtain further insight into the structure in the solid state in the absence of crystallographic data [22]. The quadrupole splitting (QS) values for triphenyltin complexes are found to be in the range 2.55–2.63 mm s^{-1} and match quite well in the range of 2.3–3.0 mm s^{-1} characteristic for a tetrahedral geometry [22,28]. This conclusion is in excellent agreement with the structures determined by X-ray crystallography (see Section 3.5). In contrast to the triphenyltin complexes, the tributyltin complexes exhibit a QS value at approximately 3.61 mm s^{-1} and the values fall in the range 3.0–4.1 mm s^{-1} specified for a trans-trigonal bipyramidal geometry with a planar Bu_3Sn unit and two apical carboxylates giving rise to polymeric structures [22,28]. Thus, the QS values strongly suggest that, in the smaller tin-bound organic substitutents (e.g. Bu_3Sn), aggregation occurs via Sn–O contacts, leading to polymeric arrays; this is in contrast to the larger tin-bound substitutents (e.g. Ph_3Sn), where such aggregation is not possible owing to steric hindrance, and hence monomeric species are found in the solid state [22]. The isomer shifts (ISs), which lie in the range 1.19–1.50 mm s^{-1}, are typical of quadrivalent organotin derivatives and the full width of half maximum ($\Gamma \pm$) of these resonance absorptions is approximately 0.85 mm s^{-1}, further suggesting the presence of a single tin centre in the complexes [28].

3.5. X-ray crystallography

The crystal structures of four of the triphenyl species have been determined. The structures conform to the

Table 5
^{13}C- and ^{119}Sn-NMR data (δ, ppm) for the triorganotin complexes in $CDCl_3$

Compound	Ligand skeleton [a]												Sn–R skeleton [b]						^{119}Sn-NMR data
	C1	C2	C3	C4	C5	C6	C1′	C2′	C3′	C4′	C5′	C6′	R	CO_2	1*	2*	3*	4*	
1	113.6	164.1	118.1	129.0	145.3	127.6	152.6	122.6	129.0	129.2	129.0	122.6	–	174.7	137.4 (646.1)	136.9 (48.6)	129.1 (64.9)	130.6 (12.5)	−88.4
2	114.2	164.1	117.8	128.6	145.0	127.5	152.5	122.6	128.8	130.2	128.8	122.6	–	174.2	16.9 (336.4)	27.7 (20.5)	26.9 (63.5)	13.6 (–)	134.8
3	112.8	163.9	117.6	128.9	145.1	125.8	149.9	137.0	130.6	129.9	127.6	115.2	17.3	174.5	137.4 (645.3)	136.3 (49.0)	128.7 (64.9)	130.0 (12.8)	−89.3
4	114.1	164.1	117.7	28.6	145.3	126.1	150.3	137.4	130.9	130.1	127.4	115.3	17.4	174.1	16.8 (352.1)	27.6 (20.9)	26.9 (64.2)	13.6 (–)	134.3
5	112.9	164.2	117.8	128.4	144.8	127.1	152.3	122.8	136.6	130.7	129.6	120.4	21.3	174.7	137.8 (640.6)	136.6 (49.0)	128.7 (64.9)	130.0 (13.0)	−91.6
6	114.3	164.7	118.2	128.9	145.3	127.8	152.9	123.3	138.5	131.2	129.1	120.8	21.8	174.7	17.3 (352.1)	28.2 (20.8)	27.4 (63.5)	14.1 (–)	130.8
7	112.8	164.1	117.7	129.5	144.8	129.2	150.3	127.5	139.9	139.9	139.9	127.5	21.3	174.8	137.3 (646.0)	136.7 (48.9)	128.9 (64.5)	130.1 (13.0)	−89.9
8	114.4	164.4	118.0	128.7	145.3	127.7	150.9	123.0	129.7	140.7	129.7	123.0	21.7	174.5	17.2 (336.4)	28.1 (20.5)	27.3 (63.5)	14.0 (–)	132.9
9	114.7	164.5	118.0	127.6	145.0	124.7	151.4	124.1	132.3	128.7	132.3	124.1	–	174.0	17.1 (335.7)	27.8 (18.8)	27.0 (63.5)	13.7 (–)	134.6
10	114.7	164.9	118.0	129.6	148.2	127.6	156.1	122.9	124.6	144.9	124.6	122.9	–	175.8	137.5 (645.9)	136.4 (48.8)	129.0 (65.0)	130.1 (12.9)	−86.9
11	114.7	165.4	118.3	129.7	148.3	127.8	155.9	123.1	124.7	145.1	124.7	123.1	–	175.9	17.1 (335.9)	27.8 (21.0)	27.0 (64.3)	13.7 (–)	138.7
12	113.1	163.6	117.8	127.3	146.7	124.3	161.4	113.8	124.8	145.0	124.8	113.8	55.0	174.7	137.2 (646.0)	136.7 (49.0)	128.9 (64.8)	130.3 (13.0)	−90.1
13	113.1	163.6	117.3	128.1	146.7	127.5	161.4	113.9	124.3	145.1	124.3	113.9	55.0	174.6	16.8 (335.8)	27.6 (20.9)	26.9 (64.9)	13.3 (–)	132.2

[a] Refer to Fig. 1 and Table 4 for numbering schemes.
[b] Numbering scheme for Sn–R skeleton as shown in Table 4. $^nJ(^{13}C–^{119/117}Sn)$ mean values are given in parentheses.

same motif and are illustrated in Figs. 2–5. Selected geometric parameters are given in Table 7. Compounds **1** and **3** are isomorphous and crystallize in the triclinic space group $P\bar{1}$ with two independent molecules comprising the asymmetric unit (labelled *a* and *b*); **5** crystallizes in the monoclinic space group $P2_1/c$ with one molecule in the asymmetric unit; and finally, **12** crystallizes in the space group $P2_1$ with four independent molecules in the asymmetric unit (labelled *a*–*d*). A careful examination of the crystallographic data did not reveal the presence of any additional symmetry in the structures [20d,e].

As indicated by the spectroscopic evidence, the molecules are monomeric in the solid state. To a first approximation the tin atom is four-coordinate, existing in a distorted tetrahedral geometry defined by a C_3O donor set. The range of tetrahedral angles for the nine molecules is 93.5(1) to 121.0(1)°, with the narrow and wide angles being ascribed to the influence of the non-coordinating O(2) atom. The O(2) atom approaches the tin atom at distances ranging from 2.752(2) Å in **1*a*** to 2.863(8) Å in **12*a***. Although not considered to represent a significant bonding interaction, the influence of the O(2) atom is such that it causes the expansion of the C(21)–Sn–C(27) angle and the concomitant contraction in the O(1)–Sn–C(15) angle. Support for the conclusion that the O(2) atom does not form a significant interaction with tin is found in the disparity in the C(1)–O(1) and C(1)–O(2) distances (Table 7). This disparity would be even greater in the absence of the intramolecular O(3)–H···O(2) interaction. Other parameters within the molecules are as expected [18,22]. The relatively small ranges observed for the geometric parameters across the series provide evidence that the variable substitution in phenyl ring B has little influence on the tin atom geometry.

Table 6
^{119}Sn Mössbauer parameters (mm s^{-1}) for the triorganotin complexes

Compound	^{119}Sn Mössbauer data [a]			
	IS	QS	Γ_1	Γ_2
1	1.19	2.55	0.90	0.87
3	1.26	2.55	0.86	0.87
5	1.28	2.63	0.88	0.89
7	1.27	2.59	0.84	0.86
9	1.50	3.61	0.87	0.88
11	1.50	3.62	0.87	0.87
12	1.28	2.63	0.86	0.86
14 [b]	1.32	2.98	0.83	0.85

[a] Parameters: QS, quadrupole splitting; IS, isomer shifts with respect to a room temperature spectrum of $CaSnO_3$; Γ_1 and Γ_2: line widths.

[b] Compound **14** is included for comparison: Ph_3SnLH (LH = 5-[(*E*)-2-(4-chlorophenyl)-1-diazenyl]-2-hydroxybenzoic acid), see Ref. [18].

Table 7
Selected geometric parameters (Å, °) for the triorganotin complexes **1**, **3**, **5** and **12**

Parameter	**1*a***	**1*b***	**3*a***	**3*b***	**5**	**12*a***	**12*b***	**12*c***	**12*d***
Sn–O(1)	2.075(2)	2.068(2)	2.070(2)	2.068(2)	2.079(2)	2.091(6)	2.063(7)	2.088(6)	2.055(6)
Sn–O(2)	2.752(2)	2.786(2)	2.773(2)	2.787(2)	2.779(2)	2.863(8)	2.835(7)	2.782(6)	2.822(6)
Sn–C(15)	2.137(3)	2.136(3)	2.136(3)	2.137(3)	2.130(3)	2.13(1)	2.11(1)	2.151(9)	2.11(1)
Sn–C(21)	2.125(3)	2.123(3)	2.124(3)	2.119(3)	2.122(3)	2.099(8)	2.14(1)	2.10(1)	2.123(9)
Sn–C(27)	2.127(3)	2.129(3)	2.123(3)	2.131(3)	2.127(3)	2.093(9)	2.122(9)	2.108(9)	2.13(1)
C(1)–O(1)	1.291(3)	1.301(3)	1.297(3)	1.300(4)	1.297(4)	1.29(1)	1.31(1)	1.31(1)	1.29(1)
C(1)–O(2)	1.249(3)	1.249(3)	1.243(4)	1.243(4)	1.246(4)	1.23(1)	1.22(1)	1.23(1)	1.25(1)
N(1)–N(2)	1.243(4)	1.239(3)	1.244(3)	1.240(4)	1.266(4)	1.23(1)	1.21(1)	1.26(1)	1.26(1)
O(1)–Sn–O(2)	52.04(4)	51.68(8)	51.76(8)	51.63(8)	51.68(7)	50.0(2)	50.9(2)	51.3(2)	51.2(2)
O(1)–Sn–C(15)	94.27(9)	94.3(1)	94.5(1)	95.6(1)	93.5(1)	94.8(3)	95.1(3)	94.0(3)	95.8(3)
O(1)–Sn–C(21)	109.7(1)	108.3(1)	109.3(1)	107.7(1)	108.2(1)	106.2(2)	110.4(3)	111.8(3)	107.7(3)
O(1)–Sn–C(27)	109.26(9)	110.5(1)	109.2(1)	110.3(1)	110.3(1)	109.6(3)	104.7(3)	107.9(3)	112.0(3)
O(2)–Sn–C(15)	146.26(9)	145.78(9)	146.23(9)	147.01(9)	144.96(9)	144.9(3)	145.9(3)	145.2(3)	147.0(3)
O(2)–Sn–C(21)	86.43(9)	85.3(1)	85.68(9)	84.60(9)	85.41(8)	83.4(3)	81.3(3)	82.6(3)	82.6(3)
O(2)–Sn–C(27)	83.31(9)	84.0(1)	84.14(9)	85.3(1)	84.19(9)	84.5(3)	82.1(3)	85.1(3)	83.7(3)
C(15)–Sn–C(21)	109.9(1)	113.1(1)	108.2(1)	113.0(1)	113.0(1)	110.1(4)	115.1(4)	113.7(4)	112.9(4)
C(15)–Sn–C(27)	110.8(1)	108.5(1)	112.3(1)	106.4(1)	108.7(1)	113.0(4)	112.5(4)	111.6(4)	113.0(4)
C(21)–Sn–C(27)	119.9(1)	119.3(1)	120.3(1)	121.0(1)	119.9(1)	120.0(4)	116.3(4)	115.7(4)	114.0(4)
Sn–O(1)–C(1)	109.3(2)	110.3(2)	109.8(2)	110.1(2)	109.8(2)	111.7(6)	110.9(6)	109.5(6)	110.9(7)
Sn–O(2)–C(1)	78.3(2)	77.6(2)	77.8(2)	77.6(2)	78.0(2)	76.3(6)	76.6(6)	78.6(5)	75.8(5)
C(6)–N(1)–N(2)	114.3(2)	114.3(3)	114.6(2)	115.1(3)	113.0(3)	112.7(9)	109.5(9)	115.1(8)	111.6(8)
N(1)–N(2)–C(8)	114.6(3)	113.7(3)	114.7(3)	114.6(3)	114.1(3)	113.6(9)	110(1)	115.9(8)	113.6(8)

The structural motif found here resembles one of the two predominant motifs for structures of the general formula $R_3Sn(O_2CR')$ although others are known [9,10]. The second motif features a polymeric array generated by the presence of bidentate, bridging carboxylate ligands. It has been argued recently, for related systems [22], that the appearance of one or other motif can be rationalised in terms of steric demands of the triorganotin residue in that bulky substituents preclude intermolecular association via Sn→O interactions. The results reported herein are consistent with this explanation.

Thus, for the series of $R_3Sn(O_2CR')$ structures where, referring to Fig. 1, the carboxylate is the ligand and the hydroxy group is in the 2′ position and a methyl group is in 5′, both the monomeric and polymeric motifs are found. For the structures with the smaller tin-bound substitutents, viz. methyl, ethyl and *n*-butyl, the polymeric motif with five-coordinate tin is found. When these were substituted for the larger groups, viz. phenyl and cyclohexyl, a monomeric structure was found with four-coordinate tin [22] as for **1**, **3**, **5** and **12**. The appearance of the two motifs was explained in terms of the competition between the formation of intramolecular Sn→O interactions, leading to a polymeric array, and other, notably, π···π interactions [22]. The respective crystal lattices are stabilized by a variety of intermolecular interactions including C–H···O, C–H···(centroid of aromatic ring) and π–π base stacking.

In **1**, centrosymmetrically related pairs of **1*a*** aggregate such that the two carboxylate ligands are 'face-to-face', being associated via π–π interactions between rings A and B (Fig. 1) such that the distance between the ring centroids is 3.88 Å, the dihedral angle is 7.7° and the symmetry operation is $1-x, 1-y, z$; the analogous parameters for **1*b*** are 4.07 Å, 9.8°, and $2-x, 1-y, 1-z$. A similar situation pertains in the lattice of **3**: for **3*a*** the distance between the ring centroids of A and B is 3.72 Å, the dihedral angle between them is 3.5° and the symmetry operation is $2-x, -2-y, -z$; for **3*b*** these are 3.92 Å, 8.2° and $1-x, -y, 1-z$ respectively. In the structure of **5**, centrosymmetrically related pairs of carboxylate residues also face each other, but in this case the ring centroid separations are greater than 4.2 Å. The closest π–π contacts involve the tin-bound phenyl group, C(21)–C(26), with a centrosymmetrically related C(21)–C(26) ring such that the separation between the ring centroids is 3.89 Å (symmetry operation: $-x, -y, 1-z$). Thus, the shift of a methyl group from the 2- (as in **3**) to 3-position (as in **5**) on ring B induces a subtle change in the molecular packing. In **12**, no evidence for short π–π contacts is found, with the shortest separation of 4.17 Å between ring centroids being found for two tin-bound phenyl groups of different molecules. It would appear that the presence of the methoxy group in **12** is sufficient to preclude association between molecules via π–π interactions involving the carboxylate ligand, as, in the recently determined structure of the acid, no evidence for base stacking was found [19]. Of all four structures, it is noteworthy that, in the absence of significant $\pi-\pi$ interactions, **12** contains the closest contact of the type C–H···ring-centroid of 2.60 Å (the angle at H is 161.0°). The O(3) atom in all structures participates in an intermolecular contact of the type O···H–C; however, no such interactions are found for the methoxy oxygen atom in **12**. From the foregoing it is clear that, although the substitution pattern in ring B has no profound influence on the molecular geometry at tin, changes in the mode of crystal packing are apparent.

4. Supplementary material

Crystallographic data have been deposited at the Cambridge Crystallographic Data Centre with deposition numbers: 149081–149084 for complex nos. **1**, **3**, **5** and **12**. Copies of the information may be obtained free of charge from The Director, CCDC, 12 Union Road, Cambridge, CB2 1EZ, UK (fax: +44-1223-336033; e-mail: deposit@ccdc.cam.ac.uk or www: http://www.ccdc.cam.ac.uk).

Acknowledgements

The financial support of the Department of Science & Technology, New Delhi, India (Grant No. SP/S1/F26/99, TSBB), of the MURST, Italy (60%, ER), and the support of the X-ray crystallographic facility by the Australian Research Council are gratefully acknowledged.

References

[1] S.J. de Mora, in: S.J. de Mora (Ed.), Tributyltin: Case Study of an Environmental Contaminant, Cambridge University Press, London, 1996, pp. 1–20.
[2] P.E. Gibbs, G.W. Bryan, in: S.J. de Mora (Ed.), Tributyltin: Case Study of an Environmental Contaminant, Cambridge University Press, London, 1996, pp. 212–236.
[3] R.F. Bennett, in: S.J. de Mora (Ed.), Tributyltin: Case Study of an Environmental Contaminant, Cambridge University Press, London, 1996, pp. 21–61.
[4] S. Nicklin, M.W. Robson, Appl. Organomet. Chem. 2 (1988) 487.
[5] A.J. Crowe, Appl. Organomet. Chem. 1 (1987) 143.
[6] A.K. Sexena, Appl. Organomet. Chem. 1 (1987) 39.
[7] S.J. Blunden, P.A. Cusack, R. Hill, The Industrial Uses of Tin Chemicals, Royal Society of Chemistry, London, 1985.
[8] A.G. Davies, P.J. Smith, in: G. Wilkinson, F.G.A. Stone, E.W. Abel (Eds.), Comprehensive Organometallic Chemistry, vol. 2, Pergamon, Oxford, 1982, p. 519.
[9] E.R.T. Tiekink, Appl. Organomet. Chem. 5 (1991) 1.
[10] E.R.T. Tiekink, Trends Organomet. Chem. 1 (1994) 71.
[11] R.C. Poller, The Chemistry of Organotin Compounds, Academic Press, New York, 1970.
[12] A.G. Davies, P.J. Smith, Adv. Inorg. Chem. Radiochem. 1 (1980) 23.
[13] W.N. Aldridge, in: J.J. Zuckerman (Ed.), Organotin Compounds. New Chemistry and Applications. In: Advances in Chemistry Series, vol. 168, American Chemical Society, Washington, DC, 1976, p. 157.
[14] B.M. Elliot, W.N. Aldridge, J.M. Bridges, Biochem. J. 177 (1979) 461.
[15] R.G. Swisher, J.F. Vallano, V. Chandrasekhar, R.O. Day, R.R. Holmes, Inorg. Chem. 23 (1984) 3147.
[16] J.F. Vallano, R.O. Day, D.N. Rau, V. Chandrasekhar, R.R. Holmes, Inorg. Chem. 23 (1984) 3153.
[17] M. Gielen, R. Willem, M. Biesemans, M. Boualam, A. El Khloufi, D. de Vos, Appl. Organomet. Chem. 6 (1992) 287.
[18] T.S. Basu Baul, S. Dhar, N. Kharbani, S.M. Pyke, R. Butcher, F.E. Smith, Main Group Met. Chem. 22 (1999) 413.
[19] T.S. Basu Baul, S. Dhar, E.R.T. Tiekink, Acta Crystallogr. Sect. C 56 (2000) 1280.
[20] (a) D.C. Phillips, A.C.T. North, F.S. Mathews, Acta Crystallogr. 24 (1968) 351;
(b) N. Walker, D. Stuart, Acta Crystallogr. Sect. A 39 (1983) 158;
(c) P.T. Beurskens, G. Admiraal, G. Beurskens, W.P. Bosman, S. Garcia-Granda, J.M.M. Smits, C. Smykalla, The DIRDIF program system, Technical Report of the Crystallography Laboratory, University of Nijmegen, 1994;
(d) TEXSAN: Structure Analysis Software, Molecular Structure Corp., The Woodlands, TX;
(e) A.L. Spek, PLATON, a Multipurpose Crystallographic Tool, Utrecht University, Utrecht, The Netherlands 2000; http://www.cryst.chem.uu.nl/platon/;
(f) C.K. Johnson, ORTEP. Report ORNL-5138, Oak Ridge National Laboratory, TN, 1976.
[21] C.E. Hadden, G.E. Martin, V.V. Krishnamurthy, Magn. Reson. Chem. 38 (2000) 143.
[22] R. Willem, I. Verbruggen, M. Gielen, M. Biesemans, B. Mahieu, T.S. Basu Baul, E.R.T. Tiekink, Organometallics 17 (1998) 5758.
[23] J. Holeček, M. Nadvornik, K. Handlir, A. Lycka, J. Organomet. Chem. 241 (1983) 177.
[24] M. Nadvornik, J. Holeček, K. Handlir, A. Lycka, J. Organomet. Chem. 275 (1984) 43.
[25] A. Lycka, J. Holeček, M. Nadvornik, K. Handlir, J. Organomet. Chem. 280 (1985) 323.
[26] J. Holeček, K. Handlir, M. Nadvornik, A. Lycka, J. Organomet. Chem. 258 (1983) 147.
[27] A. Lycka, M. Nadvornik, K. Handlir, J. Holeček, Collect. Czech. Chem. Commun. 49 (1984) 2903.
[28] R. Barbieri, F. Huber, L. Pellerito, G. Ruisi, A. Silvestri, in: P.J. Smith (Ed.), Chemistry of Tin: ^{119}Sn Mössbauer Studies on Tin Compounds, Blackie, London, 1998, pp. 496–540.